STEM CELLS TRANSLATIONAL MEDICINE™

FETAL AND NEONATAL STEM CELLS

Multipotent Stromal Stem Cells from Human Placenta Demonstrate High Therapeutic Potential

IGOR NAZAROV,[a]* JAE W. LEE,[b]* ERIC SOUPENE,[a] SARA ETEMAD,[a] DERRICK KNAPIK,[a] WILLIAM GREEN,[a] ELIZAVETA BASHKIROVA,[a] XIAOHUI FANG,[c] MICHAEL A. MATTHAY,[c] FRANS A. KUYPERS,[a] VLADIMIR B. SERIKOV[a]

Key Words. Adult stem cells • Cytokines • Mesenchymal stem cells • Placenta • Telomerase

[a]Children's Hospital Oakland Research Institute, Oakland, California, USA; [b]Department of Anesthesiology and [c]Cardiovascular Research Institute, University of California, San Francisco, California, USA

*Contributed equally as first authors.

Correspondence: Vladimir B. Serikov, M.D., Ph.D., Children's Hospital Oakland Research Institute, 5700 Martin Luther King Jr. Way, Oakland, California 94609, USA. Telephone: 510-428-3885, ext. 2480; Fax: 510-450-7910; e-mail: vserikov@chori.org

Received September 6, 2011; accepted for publication April 2, 2012; first published online in SCTM *EXPRESS* May 8, 2012.

©AlphaMed Press
1066-5099/2012/$20.00/0

http://dx.doi.org/10.5966/sctm.2011-0021

ABSTRACT

We describe human chorionic mesenchymal stem cell (hCMSC) lines obtained from the chorion of human term placenta with high therapeutic potential in human organ pathology. hCMSCs propagated for more than 100 doublings without a decrease in telomere length and with no telomerase activity. Cells were highly positive for the embryonic stem cell markers OCT-4, NANOG, SSEA-3, and TRA-1–60. In vitro, cells could be differentiated into neuron-like cells (ectoderm), adipocytes, osteoblasts, endothelial-like cells (mesoderm), and hepatocytes (endoderm)—derivatives of all three germ layers. hCMSCs effectively facilitated repair of injured epithelium as demonstrated in an ex vivo-perfused human lung preparation injured by *Escherichia coli* endotoxin and in in vitro human lung epithelial cultures. We conclude that the chorion of human term placenta is an abundant source of multipotent stem cells that are promising candidates for cell-based therapies. STEM CELLS TRANSLATIONAL MEDICINE *2012;1:359–372*

INTRODUCTION

We have recently shown for the first time that human term placenta is an abundant source of hematopoietic stem cells [1], extending earlier findings in mouse [2] to humans. Our observations have been corroborated by other groups [3, 4]. In addition to hematopoietic stem cells, placenta harbors multiple types of different stem cells that have not been appreciated yet by the field of regenerative medicine. It is now established that embryonic, fetal, and adult stem cells are maintained by different self-renewal programs [5], which change over time. Cells of the placenta are fetal. Therefore, preservation of placenta at birth would provide a once-in-a-lifetime opportunity to preserve "young" autologous stem cells. Although some stem cells that express embryonic stem cell markers and high telomerase activity are found in amniotic fluid [6], cell numbers are too low to be useful for transplantation. Another source of mesenchymal stem cells (MSCs), although rarely used, is human placenta itself [7, 8]. Previous investigations demonstrated that multipotent, multilineage cells are present in amniotic membranes of the human placenta [9]. Amniotic MSCs have been characterized in several publications [10–13]. The expression of embryonic stem cell markers has been described in amniotic cells [14–17]. Differentiation of amniotic cells toward different lineages has been described [18], and evidence of engraftment in animals has been detected [19].

The chorion makes up the predominant mass fraction of the placental outer membrane surrounding the fetus. Descriptions of chorionic MSCs are limited [20]. Thus, there is limited information on chorionic stem cells from placenta. Clonally derived MSCs from chorion have not been described, and human chorionic MSCs (hCMSCs) have not been shown to differentiate into cells of all three germ layers. The therapeutic potential of placental cells in relevant human models of disease also has not been studied.

The goal of this study was to obtain and characterize stromal stem cells from the chorion of human term placenta. The first aim was to determine whether cells expressing primitive stem cell markers were present in chorion of human term placenta, and if so to derive chorionic stromal cell lines and characterize their phenotype, differentiation potential, and marker expression, including telomerase activity and telomere length. The second aim was to demonstrate their therapeutic potential to repair injured lung in an ex vivo-perfused human lung preparation and in lung epithelial cultures and to characterize their paracrine activity.

Materials and Methods

Placenta Perfusion

Ten human placentas of male newborns were used as described earlier [1]. Following institutional review board approval, placentas were harvested from healthy females undergoing elective Cesarean section at Alta Bates Hospital (Berkeley, CA). Placentas were rinsed from the outside with saline and infused with 30 ml of an anticoagulant/vasodilator solution (Heparin sodium, 30 U/ml [Abraxis Pharmaceutical Products, Schaumburg, IL, http://www.apppharma.com]; papaverine hydrochloride, 0.25 mg/ml) at room temperature. The arteries and vein of the umbilical cord were subsequently cannulated with sterile polyethylene catheters (3-mm internal diameter), and connected to a sterile perfusion circuit, containing a heat exchange unit (Trillium-Myotherm-XP; Medtronic, Minneapolis, MN, http://www.medtronic.com), calibrated Sarns roller pump (Terumo Cardiovascular Systems Co., Ann Arbor, MI, http://www.terumocvs.com), and plastic perfusion reservoir (1 l volume). Before perfusion with the medium/albumin solution, placentas were perfused for 10 minutes with phosphate-buffered saline (PBS) to remove cord blood remaining in the placental tissue. Small leaks were stopped by placement of surgical sutures at the site of a leak. Perfusion was carried out intermittently at volume flow rate 50–100 ml/minute, arterial inflow pressure 100–120 mmHg (controlled by pressure transducers), and near zero outflow pressure in the umbilical vein. Perfusate in the reservoir was constantly oxygenated by gas mixture (5% CO_2, 95% O_2) by bubbling. Constant temperature of the perfusate (37°C) was maintained by a heat exchange unit located in the arterial line.

hCMSC Isolation

For the purpose of minimizing enzyme use, part of the placenta (approximately 10% of total chorionic plate) was isolated with clamps; arterial vessel then was perfused with 100 ml Ca^{2+},Mg^{2+}-free PBS with 100 U/ml penicillin/100 μg/ml streptomycin/0.25 μg/ml Fungizone (PSF) (Invitrogen, Carlsbad, CA, http://www.invitrogen.com), 2.5 U/ml dispase, and trypsin (2.5 mg/ml)/EDTA (Sigma-Aldrich, St. Louis, http://www.sigmaaldrich.com) for 10–20 minutes at 37°C. Following perfusion with enzymes, tissue samples were carefully dissected from the chorion to ensure complete isolation of a sample from amniotic membrane, amniotic mesenchyme, and decidual membrane. Samples (1–5 g) were then thoroughly washed in three changes of sterile PBS (100 ml) with PSF, 30 U/ml Heparin, cut into 1 × 3 × 3-mm pieces and placed in 10× by volume PBS with 0.1% collagenase I (Sigma-Aldrich) and 2.5 U/ml dispase for 30 minutes at 37°C. Tissue samples were then vortexed for 5 minutes, and the volume was adjusted to 15 ml. Samples were centrifuged at 800 rpm for 5 minutes in 15-ml tubes, and the intermediate fraction (5 ml) was aspirated. The intermediate fraction was filtered through a 100-μm-pore filter, washed twice in PBS, and filtered again through a 70-μm-pore filter. Total nucleated cells were counted, and cells were placed in 24- or 96-well plates at a density of 10^4 total nucleated cells per cm^2 in α-minimal essential medium (α-MEM) with 15% fetal bovine serum (FBS) (catalog no. SH 30088; HyClone, Logan, UT, http://www.hyclone.com), 2 mM L-glutamine, and PSF. Cultures were washed 3–5 times with PBS after 3 days to isolate nonadherent cells from plastic-adherent colonies, which were further cultured up to 3 weeks with weekly medium change.

Embryoid body-like growth of colonies, attached to plastic, was usually found after 5–7 days of incubation. These three-dimensional structures, representing single colonies, were lifted by micropipette under visual control of a ×5 microscope objective and placed on plastic, collagen, or Matrigel (catalog no. 356234; BD Biosciences, San Diego, CA, http://www.bdbiosciences.com) for further growth in α-MEM with 10%–15% FBS, 2 mM L-glutamine, and PSF. Following initial growth of isolated primary colony to obtain 100–500 cells, primary colonies (passage 0) were then further passaged in T25 flasks. The first two passages were performed with the cells reaching approximately 70%–90% confluence by splitting the cells 1:1. For further passages, cells were split at a 1:4–1:8 ratio and propagated for up to 55 passages.

Differentiation of hCMSCs

The confluent primary cultures were washed twice with PBS without Ca^{2+} or Mg^{2+} (Invitrogen). Cells were detached following digestion with trypsin/EDTA and then resuspended in medium and cultured in culture flasks (Costar, Corning Life Sciences, Acton, MA, http://www.corning.com/lifesciences) or 12-well clusters. Adipogenic differentiation was stimulated by seeding the cells for 3 weeks in medium supplemented with 10^{-8} ml/l dexamethasone and 5 μg/ml insulin. To confirm adipocyte differentiation, fat in cells was stained with an Oil Red (Sigma-Aldrich) ethanol/water solution. Osteogenic differentiation was induced by culturing in medium containing 10 mM β-glycerol phosphate, 50 μg/ml ascorbic acid, and 10^{-8} ml/l dexamethasone for 3 weeks. To confirm osteogenic differentiation, calcium precipitates in cells were determined using alizarin red staining (Sigma-Aldrich). Additional cells were tested to differentiate into endothelial cells in Methocult medium (StemCell Technologies, Vancouver, BC, Canada, http://www.stemcell.com) and on Matrigel (BD Biosciences) coating. Formation of capillary networks on Matrigel and expression of endothelial markers in differentiated cells (CD31, vascular endothelial growth factor receptor [VEGFR]) were performed by immunofluorescence. Ectodermal differentiation into neuronal-like cells was done by addition of retinoic acid (5×10^{-8} M to the medium) and 10^{-8} M nerve growth factor (NGF). Differentiation was confirmed by immunostaining for neuronal markers nestin and Neurofilament-200. Endodermal differentiation was done by directing cells into hepatocyte-like cells. Hepatic differentiation was done by culture in medium containing α-MEM, 12% fetal bovine serum (FBS), 2 mM L-glutamine, 10 mM *N*-acetyl-L-cysteine, 20 ng/ml hepatocyte growth factor (HGF), 10 ng/ml oncostatin, 10^{-7} M dexamethasone, 10 ng/ml fibroblast growth factor (FGF)-4, and ITS (insulin, transferrin, selenium). Differentiation into hepatocytes was confirmed by staining for human albumin and α-fetoprotein.

Analysis of Cell Survival and Cell Proliferation

For the trypan blue assay, cells were plated (10^4 cells per cm^2) for 36–72 hours. After being washed with PBS, cells were stained with 0.2% trypan blue (Sigma-Aldrich), and positive (dead) cells were counted in randomly selected three fields in binocular microscope (at least 300 cells per single view). To determine cell doubling time, cells were counted, plated for 48–72 hours and

lifted by trypsin/EDTA, and cell numbers were counted and plotted on a $\log_2$ scale.

Immunostaining

Immunostaining protocols were described by us before [1]. Paraffin-embedded tissue samples of placenta were stained for markers of human stem cells following fixation by perfusion in 4% paraformaldehyde. Paraffin sections were first deparaffinized in xylene (Sigma-Aldrich) and then rehydrated in alcohols. Cultured cells were fixed with 2.4% paraformaldehyde, washed in PBS, and permeabilized with cold methanol (−20°C) and 1% Triton X-100 for 5 minutes (when required for intracellular antigen staining). Antigen retrieval was done by digestion with proteinase K (20 U/ml) in Tris/EDTA buffer for 2 minutes at room temperature. Slides were then washed, incubated with blocking buffer (3% bovine serum albumin [BSA] in 4× saline-sodium citrate buffer, 2% goat serum, 3% FCS, 0.1% Tween 20) for 60 minutes at 37°C, and then incubated with primary antibody (1:100 dilution) overnight at 4°C. Slides were washed, incubated with blocking solution for 20 minutes, and then incubated with secondary antibody (1:400) labeled with fluorescein isothiocyanate or Alexa Fluor 633 for 60 minutes at 37°C, washed, and mounted on glass with Gold Antifade reagent (Invitrogen). The list of specific antibodies used for immunostaining and Western blot analyses is given in the supplemental online data.

Western Blot Analyses

Western blots were performed for several proteins with reference to actin. Cells were scraped off to a cold lysis buffer composed of 1% Triton X-100, 2 mM EDTA, 2 mM dithiothreitol, 0.25 mg/ml leupeptin, 0.25 mg/ml pepstatin A, 0.4 mg/ml aprotinin, and 0.1 mM phenylmethylsulfonyl fluoride. In cell culture experiments, samples from three cell sheets were combined in 100 μl of ice-cold buffer. Protein content of the lysate was measured by the bicinchoninic acid assay method (Pierce Endogen, Thermo Fisher Scientific Inc., Rockford, IL, http://www.piercenet.com). Samples (20 μg total protein) were separated on 10% SDS-polyacrylamide gels, and then separated proteins were transferred to membranes, where they were blocked overnight at 4°C with 5% nonfat dry milk in TBST (10 mM TrisCl, pH 8.0; 150 mM NaCl; 0.1% Tween 20). The blot was rinsed twice with TBST and incubated for 2 hours at room temperature with the appropriate antibody in TBST containing 5% BSA. The membrane was washed for 15 minutes with TBST and incubated with goat anti-mouse IgG conjugated with horseradish peroxidase in 5% milk for 1 hour, and then washed three times with TBST and developed with enhanced chemiluminescence reagent (Amersham Biosciences, Arlington, IL, http://www.amersham.com).

Culture Experiments with Calu-3 Bronchoepithelial Cells, Permeability Measurements, and Coculture

To determine whether the chorionic stem cells are capable of facilitating epithelial repair, layers of Calu-3 lung bronchoepithelial cells (HTB-85; American Type Culture Collection [ATCC], Manassas, VA, http://www.atcc.org) were grown at the air-liquid interface on inserts of the Transwell support systems (Sigma-Aldrich). Calu-3 cells form tight junctions in vitro, thus allowing the measurement of barrier functions of epithelium. The methods used to determine permeability of Calu-3 epithelial sheets, permeability to albumin, and estimation of transepithelial electrical resistance are described in details by Serikov et al. [21]. Transepithelial electrical resistance (TER; a measure of tight junctional ion permeability) was measured using the EVOM-METER (World Precision Instruments, Sarasota, FL, http://www.wpiinc.com). Calu-3 cells were grown on 0.4 μm-pore Costar filters in Dulbecco's modified Eagle's medium (DMEM)/Hanks' F12 medium with 10% FBS and an array of growth factors [21]. After 10–12 days of culture, confluence was reached and cell layers achieved a TER of 800–1,200 $\Omega \times cm^2$. To damage cells, layers were exposed to hydrogen peroxide solution (2 mM) for 5 minutes. Two hours later, hCMSCs, bone marrow-derived MSCs (BM-MSCs), or A549 (human lung carcinoma epithelial cell line ATCC CCL-185, negative control) were either applied to the apical side or added to the lower well of the Transwell system (basolateral side) at a concentration of 10^5 cells per cm^2. TER was measured in 12-hour periods for 24–48 hours. Experiments were performed in four to six separate cell cultures, and the results were averaged. Human mesenchymal bone marrow-derived stem cells were obtained from the laboratory of Dr. D. Prockop, Tulane University (New Orleans, LA).

Reduction of Growth Factors Production by Small Interfering RNA in Placental Cells

RNA silencing was done using transfection reagents and company-made small interfering RNA (siRNA) from Dharmacon, Inc. (Lafayette, CO, http://www.dharmacon.com), according to the manufacturer's instructions. Placental hCMSCs at passages 5–8 (1×10^6 cells) were cultured without serum for 6 hours in Opti-MEM (Gibco, Grand Island, NY, http://www.invitrogen.com), treated with siPORT NeoFX (a lipid-based reverse transfection agent; Ambion, Austin, TX, http://www.ambion.com) and the siRNAs for keratinocyte growth factor (KGF), HGF, and basic fibroblast growth factor (bFGF) were applied separately or as combination of all the above for 24 hours. Effectiveness of transfection and optimal dilution of siRNA was determined and confirmed by fluorescent microscopy using red-fluorescent siRNA probes from the same company. Noncoding siRNA provided by the same manufacturer was used as a negative control. The medium was then replaced before cells were used in coculture experiments.

Enzyme-Linked Immunosorbent Assay

The levels of secreted chorionic gonadotropin, HGF, FGF, KGF, and angiopoietin-1 proteins in cell culture media were measured using standard enzyme-linked immunosorbent assay kits (RayBiotech, Norcross, GA, http://www.raybiotech.com; R&D Systems Inc., Minneapolis, http://www.rndsystems.com) according to the manufacturers' instructions.

Ex Vivo-Perfused Human Lung and Measurement of Alveolar Fluid Clearance

Human donor lungs (preserved at 4°C for 4–8 hours) that were declined for transplantation by the California Transplant Donor Network as previously described were used [22]. On arrival, the right lung was separated, and the pulmonary artery was cannulated by passing a Foley catheter 2–3 cm into the surgical stump, securing it in place with a purse-string suture. The Foley catheter was then connected to a peristaltic pump. To measure pulmonary artery pressure, a pulmonary artery catheter was passed through a side port in the tubing and advanced to the end of the

Foley catheter. The right mainstem bronchus was then intubated. The lung preparation was then weighed and suspended within a sealed acrylic container from a mass transducer (Harvard Apparatus, Holliston, MA, http://www.harvardapparatus.com). The container was surrounded by a heated (38°C) water bath, where the inner container served as a reservoir for the perfusate solution (DMEM H-21 with 5% albumin, 900 ml). The lung preparation was slowly warmed for 1 hour with the peristaltic pump until a perfusion flow rate of 0.3–0.4 l/minute was achieved, giving an average mean pulmonary artery pressure of 10–12 mmHg. Venous drainage was passive at near zero pressure. When the temperature of the venous drainage reached 36°C, the lung was slowly inflated with continuous positive airway pressure at 10 cmH_2O with 95% O_2 and 5% CO_2. Pulmonary artery pressure and lung weight were continuously monitored using a computer-integrated data acquisition system (Biopac, Santa Barbara, CA, http://www.biopac.com). One hour after perfusion, the right upper lobe (RUL) was then cannulated with a polyethylene catheter (240 tubing; Becton, Dickinson and Company, Franklin Lakes, NJ, http://www.bd.com), which was advanced until gentle resistance was encountered. Warmed normal saline with 5% albumin (125 ml, alveolar fluid solution) was then instilled into the RUL. Alveolar fluid clearance (AFC) was calculated by the change in the total protein concentration of the RUL aspirate over time, using the following equation: AFC (%/hour) $= 1 - C_i/C_f$ (where C_i is protein concentration at time 0 and C_f is protein concentration after 1 hour). One hundred milliliters of fresh whole human blood containing approximately 260×10^6 neutrophils was added to the perfusate, and 10 ml of alveolar fluid solution containing 6 mg of endotoxin (0.1 mg/kg) was instilled into the right middle lobe (RML). For experiments involving intrapulmonary delivery of hCMSC, 5×10^6 hCMSCs grown in tissue culture were suspended in 20 ml of warm PBS and slowly instilled into the RML 1 hour after the instillation of 6 mg of endotoxin. For controls, 5×10^6 normal adult human lung fibroblasts (PromoCell, Heidelberg, Germany, http://www.promocell.com) were used. After 4 hours, AFC in the RML was measured by the same procedure as described above for RUL. Samples of alveolar fluid from RUL and RML were taken to determine neutrophil count and concentration of cytokines by enzyme-linked immunosorbent assay.

Isolation of Primary Cultures of Human Alveolar Epithelial Type II Cells

Type II epithelial cells were isolated from human lung. For isolation, a lobe was selected by gross inspection that was free of obvious consolidation or hemorrhage. The pulmonary artery was perfused 10 times with PBS, and the distal airspaces were then lavaged 10 times with Ca^{2+},Mg^{2+}-free PBS solution containing 0.5 mM EGTA and 0.5 mM EDTA. Elastase (13 U/ml in Ca^{2+},Mg^{2+}-free Hanks' balanced salt solution), was instilled into the distal airspaces through segmental bronchial intubation, and the lobe was incubated in a water bath at 37°C for 45 minutes. Following digestion, the lobe was minced finely in the presence of FBS and DNase, 500 μg/ml. The cell-free fraction was filtered sequentially through one layer of sterile gauze, two layers of gauze, and 150- and 30-μm nylon meshes. The filtrate was then layered onto a Percoll density gradient (1.04–1.09 g/ml) and centrifuged at 1,500 rpm for 20 minutes. The top layer, containing both type II pneumocytes and macrophages, was collected and centrifuged at 800 rpm for 10 minutes. The cell pellet was resuspended in Ca^{2+},Mg^{2+}-free PBS solution containing 5% FBS and incubated with magnetic beads coated with anti-CD14 antibodies at 4°C for 40 minutes. Macrophages were then selectively depleted with a Dynal magnet (Dynal Biotech, Oslo, Norway, http://www.invitrogen.com/dynabeads) and further incubation on Petri dishes coated with human IgG antibodies against macrophages. The remaining alveolar epithelial type II cells were then plated on collagen I-coated 24-well Transwell plates (0.4 μm pore size, polytetrafluoroethylene membrane; Costar, Corning) at 5% CO_2, at 37°C at a concentration of 1.0×10^6 cells per well. The cells were exposed to media, DMEM-H21 and Hanks' F12 medium (1:1), with antibiotics (penicillin, streptomycin, gentamicin, and amphotericin) and 10% FBS for 48 hours and without FBS for 24 hours. Seventy-two hours after the isolation, the type II cells were washed once with PBS and then exposed to a mix of cytokines (interleukin-β [IL-β], tumor necrosis factor-α [TNFα] and interferon-γ [cytomix]) at a concentration of 50 ng/ml for 24 hours. For experiments involving hCMSCs, hCMSCs (250,000 cells per well) were added to the bottom chamber of the Transwell plate simultaneously with the cytomix.

Fluid Transport Across Human Alveolar Epithelial Type II Cells

Net fluid transport was measured across human type II cells on Transwell plates (0.4 μm pore size and collagen I-coated; Costar, Corning) in a humidified tent within a 37°C, 5% CO_2 incubator with 100% humidity. Measurement of fluid transport from the apical to the basolateral membrane of the type II cell monolayers was done at 120 hours after the initial isolation and 48 hours after the air-liquid interface was achieved (transmembrane electrical resistance peaked at approximately 1,500 $\Omega \times cm^2$ at 96 hours). The cells were first exposed to 150 μl of cytomix (containing 0.3 μCi/ml of ^{131}I-albumin) in the apical chamber of the Transwell with and without hCMSCs in the bottom chamber. After 5 minutes, 20 μl of the medium was then aspirated as the initial sample. After 24 hours, another 20 μl was aspirated from the upper compartment of the Transwell as the final sample. Each sample was weighed, and radioactivity was counted in a gamma counter (Minaxi 5000 series; Packard BioScience/PerkinElmer Life and Analytical Sciences, Waltham, MA, http://www.perkinelmer.com). Net fluid transport was calculated as described in [22].

Fluorescence-Activated Cell Sorting Analysis

Cells were trypsinized, immunostained, and analyzed using a FACSCalibur flow cytometer (BD Biosciences) and FlowJo analysis software (Tree Star, Ashland, OR, http://www.treestar.com). Antibodies directed against human CD31, CD45, CD73, CD90, CD105, CD117, CD133, HLA-DR, TRA-1–60, and SSEA-3/4 were used to characterize cells in hCMSC cultures.

Measurement of Telomerase Activity and Telomere Length

Telomerase activity was measured by telomere repeat amplification protocol (TRAP) with the TRAPeze Telomerase Detection Kit (S7700; Chemicon, Temecula, CA, http://www.chemicon.com) according to the manufacturer's protocol. Briefly, 10^5–10^6 cultured cells were lysed in 0.2 ml of CHAPS buffer (3-[(3-cholamidopropyl)-dimethylammonio]-1-propane sulfonate), and 0.2–1 μg of cell extract protein was used in TRAP assay. The extended and amplified TRAP products were resolved on 12.5%

nondenaturing polyacrylamide gel. The relative telomerase activity was determined by the densitometry analysis of TRAP reaction products in relation to its telomerase control, 36-bp polymerase chain reaction (PCR) amplification internal control, and the TRAP signals for telomerase-positive standard cell extract. Telomere length was determined by terminal restriction fragment (TRF) analysis with the TeloTAGGG Telomere Length Assay Kit (Roche Applied Science, Indianapolis, https://www.roche-applied-science.com). Isolated genomic DNA (1–2 μg) was digested with a HinfI/RsaI enzyme mixture for 12–16 hours at 37°C. Then, the DNA samples were resolved by 0.6% agarose gel electrophoresis. Gels were Southern blotted to a positively charged nylon membrane (Hybond N+; Amersham), which was then hybridized with a digoxigenin (DIG)-labeled probe specific for telomeric repeats and incubated with a DIG-specific antibody covalently coupled to alkaline phosphate. TRF lengths were estimated by densitometry analysis of the Southern blot images.

Fluorescence In Situ Hybridization for Human Y Chromosome

The probe for the human Y chromosome was purchased from Cambio (Dry Drayton, U.K., http://www.cambio.co.uk), and staining was done according to the manufacturer's instructions. Slides with tissue for fluorescence in situ hybridization (FISH) were first incubated with sodium thiocyanate solution for 10 minutes at 80°C. Then, the slides were treated with pepsin solution for 2–4 minutes 37°C, quenched in glycine and washed in PBS, and then postfixed in 2% paraformaldehyde solution. Once washed, the samples were dehydrated through graded alcohols. The prediluted Cambio Y chromosome paint probe was applied, and slides were then hybridized at 80°C for 60 minutes. The slides were washed using a formamide solution at 37°C for three changes of 5 minutes each, washed in PBS, and mounted with 4′,6-diamidino-2-phenylindole or SYBR Green (Invitrogen) to stain the nuclei.

Reverse Transcription and Real-Time PCR

Total RNA of hCMSC lines 3, 22, and 22C (a derivative of line 22); the human diploid fibroblast strain IMR90; human embryonic stem cell (hESC) line H-9; and human induced pluripotent stem cells (iPSCs) were extracted using ToTALLY RNA kit (Ambion) following the manufacturer's instructions. Trace amounts of DNA in the RNA preparation was removed by treatment with TurboDNase (Ambion). DNA-free RNAs were extracted with phenol-chloroform and concentrated by ethanol precipitation. No-RT control PCRs were performed with iTAQ SYBR Green Supermix (Bio-Rad, Hercules, CA, http://www.bio-rad.com) using a human *ACTB* primer pair (catalog no. PPH00073E; Qiagen, Valencia, CA, http://www1.qiagen.com) on an ABI7000 instrument. RNA samples were considered DNA-free when no signal was detected at C-threshold values less than 35 for a 40-cycle amplification program. Semiquantitative expression of *POU5F1* (protein OCT-4) and *NANOG* was determined as follows. RNA was reverse transcribed with iSCRIPT Select cDNA Synthesis kit (Bio-Rad) in the presence of random primers in 20 μl. An equal volume of cDNAs, 1 μl, was amplified with High-Fidelity Platinum Taq Polymerase (Invitrogen) for 30 cycles in presence of gene-specific primer set for *POU5F1* (protein OCT-4), *NANOG*, and *GAPDH* (supplemental online Table 1).

Quantification of gene expression was analyzed using gene-specific RT^2 qPCR Primers (Qiagen) for *POU5F1* (protein OCT-4) (catalog no. PPH02394E) and *NANOG* (catalog no. PPH17032E) with *GAPDH* (catalog no. PPH00150E) as reference. Real-time PCRs were performed with 0.5 μl of cDNA per reaction and 400 nM gene-specific RT^2 qPCR Primer, using iTAQ SYBR Green Supermix with ROX (Bio-Rad). Reactions were performed in triplicate in a 13-μl volume in a 96-well plate format and were run on an ABI7000 instrument (Applied Biosystems, Foster City, CA). Values normalized to *GAPDH* were obtained in hESCs, iPSCs, and hCMSCs and were compared with the normalized values obtained for IMR90 fibroblasts. Expression of both genes was detected under our condition by quantitative PCR. The $\Delta\Delta C_t$ method was used to determine the fold change in expression relative to IMR90. Additional details of methods and primer sequences are given in supplemental online Table 1.

Acute Cell Toxicity and Tumorigenicity Studies in Mice

NOD/SCID mice were obtained from the Jackson Laboratory (Bar Harbor, ME, http://www.jax.org). All mice received 1.5–2.5 Gy of whole body irradiation. In 20 mice, injection of 0.25×10^6 hCMSCs was done under i.v. general anesthesia, and injection of 10^6 hCMSCs was done i.p. Mice were observed closely for 12 hours following recovery from anesthesia and then followed for up to 12 months. At autopsy, special care was taken to determine the presence of tumors in all organs. To test for teratoma formation, 1 million cells were injected locally into the leg muscle in 10 animals. In 50% of the animals, hCMSCs were grown on Matrigel prior to injection. Histology was done after 6–12 months at the site of cell injection.

Engraftment of hCMSCs in Chimeric Mice

Immunodeficient NOD/SCID mice received 1.5–2.5 Gy of whole body irradiation followed by i.p. injection of 10^6 hCMSCs. Two to 6 months following transplantation, animals were sacrificed, and samples of blood, bone marrow, muscle, heart, lung, kidney, intestine, liver, and spleen cells were harvested. Samples of tissues were analyzed by FISH using human Y chromosome probe (Cambio) according to the manufacturer's protocol and immunostained for appropriate human tissue-specific antigens. Samples of tissue were analyzed for the presence of human β-globin gene by PCR. Detection of human genomic DNA was performed by PCR amplification of the human β-globin gene (*HBB*; geneID: 3043). Sequences of primers are available upon request.

Statistical Analyses

Statistical analysis was performed using analysis of variance (ANOVA) and the Mann-Whitney-Wilcoxon test. All experiments were run at least in triplicate, and results are presented as mean $\pm$ SD. In experiments where the data were not normally distributed, they were log-transformed and compared using the ANOVA test with Bonferroni adjustment if appropriate, or they were compared using the Wilcoxon rank sum test with Bonferroni adjustment without log-transformation. Stata 9.0 (StataCorp, College Station, TX, http://www.stata.com) was used for statistical analysis. Results were considered to be statistically significant if $p < .05$.

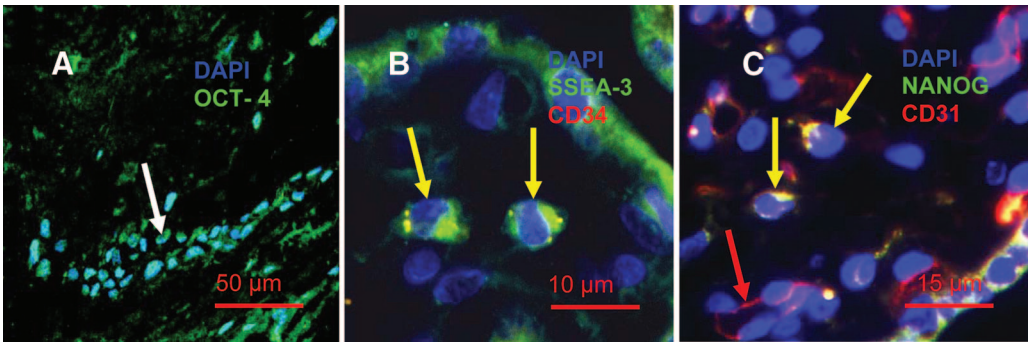

Figure 1. Multiple clusters of cells positive for embryonic stem cell markers are present in chorion. **(A):** Clusters of OCT-4-positive cells in chorionic stroma. Paraffin section of human placenta, stained for OCT-4 (fluorescein isothiocyanate [FITC], green) and nuclei (DAPI). Merged image. OCT-4 was highly expressed in nuclei of cells (white arrow). **(B):** SSEA-3-positive cells (FITC, green) and CD34-positive cells (AF633, red) in placental chorionic stroma (arrows). Nuclei are blue (DAPI). Merged image. **(C):** Dual staining for NANOG (FITC, green) and CD31 (AF633, red). NANOG-positive cells were present in chorionic stroma (yellow arrows), and capillaries stained positive for CD31 (red arrow). Nuclei are blue (DAPI). Merged image. Split images and control for isotype antibody are shown in supplemental online Figure 1. Abbreviation: DAPI, 4′,6-diamidino-2-phenylindole.

RESULTS

Cells with Markers of Pluripotency in Chorion of Human Term Placenta

Populations of OCT-4-, NANOG-, and SSEA-3-positive cells that reside inside the chorionic stroma of placental tissue were identified immunohistologically. Figure 1 and supplemental online Figure 1 illustrate clusters of OCT-4-positive cells, as well as SSEA-3- and NANOG-positive cells in the chorionic stroma. These results indicate that primitive stem cells with an embryonic stem cell-like phenotype are present in the placental chorionic stroma.

Chorionic Stem Cell Lines

Plastic-adherent hCMSC lines were obtained from all 10 placentas (supplemental online Fig. 2A, 2B). Several lines isolated from three-dimensional spherical structures were obtained from four selected placentas. Such spherical "mushroom"-like structures were attached to substrate only at the base and resembled embryoid bodies in overall appearance, as illustrated in supplemental online Figure 2C and 2D. The typical morphologies of these cell lines at different passages and plating densities are shown in supplemental online Figure 2. Lines obtained from three-dimensional spherical structures also demonstrated rapid development of embryoid bodies in intermediate and late passages (supplemental online Fig. 2E). Unlike true embryoid bodies, these cells did not demonstrate spontaneous differentiation. Cells proliferated for up to 55 passages (>100 doublings) (supplemental online Table 2).

Cell lines derived from three-dimensional spherical structures expressed a variety of stem cell markers. Immunostaining of adherent cultures further demonstrated expression of NANOG, OCT-4, SSEA-3, and TRA-1–60 (Fig. 2; split confocal images are shown in supplemental online Fig. 3). Bone marrow-derived MSCs did not show expression of these markers (supplemental online Fig. 3). Of interest, high nuclear expression of Neurofilament-200, typical of fetal brain neurons, was noted in some lines. To consider different opinions regarding specificity of antibodies against OCT-4, additional staining for hCMSCs was done with monoclonal mouse antibody C-10 (Santa Cruz Biotechnology Inc., Santa Cruz, CA, http://www.scbt.com). Results are illustrated in supplemental online Figure 4. hCMSCs expressed OCT-4 by staining with C-10 antibody, whereas human bone marrow-derived MSCs did not. hESCs were used as positive control. Western blot further confirmed a high level of protein expression of embryonic stem cell markers NANOG and OCT-4, as shown in supplemental online Figure 4 with the use of rabbit polyclonal antibody against OCT-4 (Abcam, Cambridge, MA, http://www.abcam.com).

The results of quantitative analyses of expression of *NANOG* and *POU5F1* in hCMSCs in comparison with fibroblast IMR90 (negative control), human embryonic stem cell line H-9 in the form of embryoid body (EB) growth and the growth on the feeder layer (H-9), and iPSCs are shown in Figure 3. hCMSCs expressed levels of RNA for these genes approximately 100-fold more than fibroblasts and at the same levels as embryoid body-grown line H-9 (EB). As shown in supplemental online Figure 5A, fluorescence-activated cell sorting analyses indicated a high expression of TRA-1–60, SSEA-3/4, CD105, CD73, and CD117 and a lack of expression of CD45, CD133, and HLA-DR. Expression of CD105 and CD90 was also noted in attached cell cultures by immunostaining (supplemental online Fig. 5B).

Placentas were collected from male babies, and to determine the presence of fetal cells in lines, we applied FISH for the human Y chromosome in cell cultures. Cells were predominantly positive for the human Y chromosome, as illustrated in supplemental online Figure 5C. These results indicate that hCMSC lines derived by our protocol contain predominantly fetal cells, although the presence of maternal cells could not be completely ruled out.

Differentiation of hCMSC Lines In Vitro

Following a 3-week culture in adipogenic differentiation medium, cell cultures demonstrated the presence of lipid vacuoles, indicative of adipogenic differentiation, as revealed by Oil Red staining (Fig. 4A). Subsequent to a 4-week culture in osteogenic differentiation medium, cell cultures demonstrated the presence of calcium precipitates, indicative of osteoblast differentiation, as revealed by alizarin red staining (Fig. 4B). After culture on Matrigel for 1 week, hCMSCs displayed typical endothelial cell morphology for attached cells, as shown in Figure 4C. Following a 2-week culture in Methocult, cells developed complex three-dimensional networks of nonattached cells (Fig. 4D). When grown on Matrigel/Methocult media, hCMSCs expressed the endothelial cell markers CD31 and KDR (type III receptor tyrosine kinase,

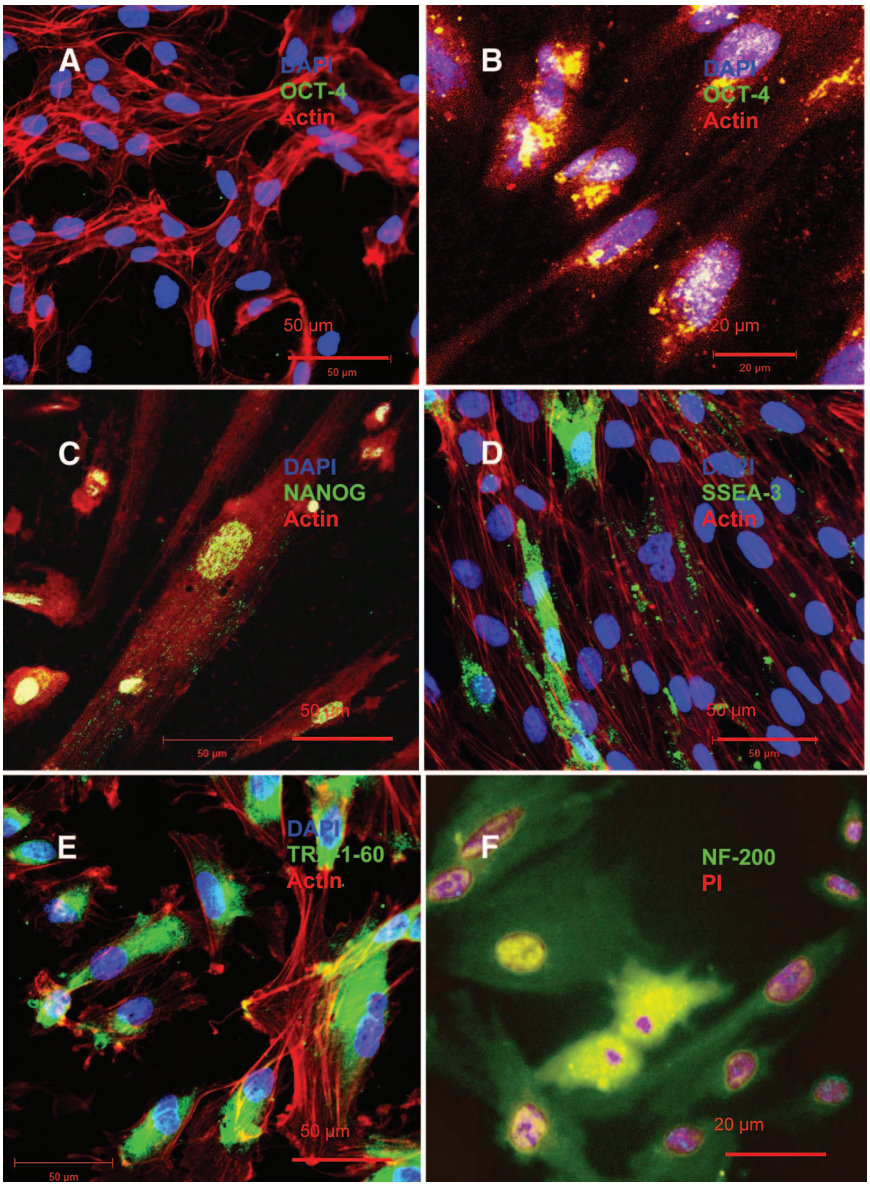

Figure 2. Chorionic stem cells express embryonic stem cell markers OCT-4, NANOG, SSEA-3, and TRA-1–60. **(A):** Phenotype characterization of chorionic mesenchymal stem cells. Fluorescent confocal microscopy merged images. **(A–E):** Nuclear costaining is DAPI (blue); actin costaining is with phalloidin-AF-568 (red). **(A):** Negative control; isotype antibody staining for NANOG and OCT-4. **(B):** Staining for OCT-4 (fluorescein isothiocyanate [FITC], green) and localization to the nuclei. **(C):** Staining for NANOG (FITC, green) and localization to the nuclei. **(D):** Staining for SSEA-3 (FITC, green). **(E):** Staining for TRA-1–60 (FITC, green). **(F):** Staining for Neurofilament-200 (FITC, green) and nuclear costaining PI (red). Abcam rabbit polyclonal antibodies against OCT-4 were used. Split images are shown in supplemental online Figure 3. Abbreviations: DAPI, 4′,6-diamidino-2-phenylindole; NF, Neurofilament; PI, propidium iodine.

also known as vascular endothelial growth factor receptor 2), as illustrated in Figure 4E–4G for substrate-adherent or outer-layer cells. Substrate-nonadherent cells grown as free-floating spheres differentiated into leukocyte lineages of blood cells, as shown by their expression of CD45 (Fig. 4E). Embryoid body-like structures, when grown on Matrigel, intensively expressed OCT-4 and CD117 in cells inside the structure, whereas cells of the outer layer did not express these markers (Fig. 4F–4H). Additional split images are shown in supplemental online Figure 6.

Endodermal differentiation was confirmed by directing cells into hepatocyte-like cells. Albumin, α-1-antitrypsin, and α-fetoprotein were first detected by immunostaining after a 3-week culture period, and expression was confirmed by reverse transcription (RT)-PCR (10–100-fold increases in expression) (supplemental online Fig. 7). Ectodermal differentiation into neuronal-like cells was accomplished by addition of retinoic acid (5×10^{-8} M to the medium) and 10^{-8} M NGF. After culture under these conditions for 3 weeks, cells demonstrated morphological characteristics of neurons (Fig. 5) and expressed Neurofilament-200 and nestin—markers of neuronal differentiation.

Telomere Length and Telomerase Activity

Different mechanisms, some involving telomerase activity, are used by cells to maintain telomere length [23]. As hCMSCs could be propagated for more than 100 doublings, expression of telomerase was monitored. For this purpose, expression of human telomerase reverse transcriptase was assessed using RT-PCR, and telomerase activity was examined using the TRAP assay. Telomerase activity in hCMSCs was undetectable when compared with the telomerase-positive human embryonic adenocarcinoma cell line NTERA-2, and with other positive and negative controls (supplemental online Fig. 8). Telomere length was determined using TRF analysis (supplemental online Fig. 8). In all hCMSC cultures, telomeres maintained long-range lengths; no differences in length were found between early and late passages.

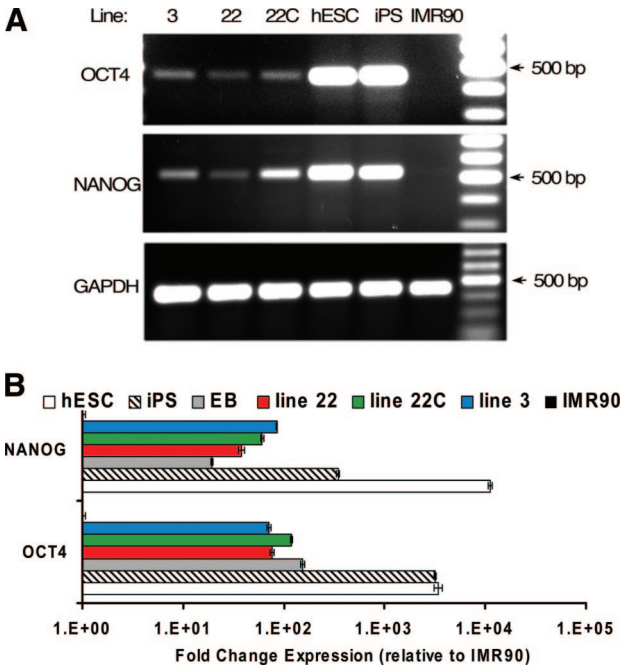

Figure 3. Chorionic mesenchymal stem cells express high amounts of RNA of *POU5F1* (OCT-4 protein) and *NANOG*. **(A):** Total RNAs were isolated from hCMSC lines 3, 22, and 22C; hESCs; IMR90-derived iPS cells; and IMR90. hESCs, line H-9, were grown either as embryoid bodies (EBs) in suspension or on a mouse feeder layer (H-9). An equal amount of RNAs were reverse-transcribed in presence of random primer, and an equal volume of cDNAs was then amplified using gene-specific primer pairs for *POU5F1*, *NANOG*, and *GAPDH*. An equal volume of the polymerase chain reactions (PCRs) was loaded on a 1.2% agarose gel, which was stained with ethidium bromide. The DNA molecular mass standard is shown on the right, and the position of the 500-bp fragment is indicated. **(B):** Quantitative analyses by real-time PCR demonstrate high levels of *POU5F1* and *NANOG* RNA in hCMSC lines. Shown is the logarithmic plot of relative *POU5F1* and *NANOG* expression. hCMSCs expressed approximately 100-fold more RNA for the *NANOG* and *POU5F1* genes as compared with IMR90 fibroblasts, and same amount as embryoid body-grown embryonic line H-9 (EB). cDNAs obtained by reverse transcription of 1 μg of total RNA, as described in **(A)**, were analyzed using gene-specific RT^2 qPCR Primers (Qiagen) for *POU5F1*, *NANOG*, and *GAPDH* and iTaq Polymerase SYBR Green. Expression of *POU5F1* and *NANOG* was normalized to the values obtained for the housekeeping gene *GAPDH*. Normalized values obtained in (hESC, ine H-9), EBs (hESC, line H-9), iPS cells (IMR90-derived), and hCMSC lines 3, 22, and 22c were calculated relative to the normalized values obtained in IMR90 cells. The $\Delta\Delta C_t$ method was used to determine the fold change in expression relative to IMR90. Abbreviations: hESC, human embryonic stem cell; iPS, induced pluripotent stem.

hCMSCs Restore AFC and Lung Epithelial Permeability in Ex Vivo-Perfused Human Lungs

Damage produced by endotoxin to the isolated perfused human lungs reduced AFC (an integrative measure of lung epithelial permeability and active sodium and fluid transport) to zero (Fig. 6) and led to a sharp increase in IL-1β, TNFα, and IL-8 levels in the alveolar fluid (supplemental online Fig. 9). Instillation of 5×10^6 hCMSCs normalized alveolar fluid clearance (Fig. 6). The neutrophil counts in bronchoalveolar lavage fluid increased in the endotoxin-injured lung lobe. On average hCMSC instillation restored neutrophil count to control levels, although not significantly by statistical analyses because of wide variations in baseline levels. Instillation of hCMSCs significantly reduced the level of IL-1β and reduced the level of IL-8 by 30% (although this difference did not reach statistical significance). The level of TNFα in the bronchoalveolar lung fluid was unchanged (supplemental online Fig. 9). hCMSCs also restored protein permeability and net fluid transport in primary cultures of human alveolar epithelial type II cells injured by an inflammatory insult with cytomix. The addition of cytomix reduced net fluid transport by $>$80% in the primary cultures. Results are illustrated in Figure 6 and supplemental online Figure 9. As shown, the simultaneous addition of hCMSCs (250,000 cells per well) to the bottom chamber of the Transwell plate partially restored normal protein permeability (Fig. 6) and net fluid transport (supplemental online Fig. 9). The addition of normal human lung fibroblasts had no significant effect on either end point. Dose-response comparative analyses between hCMSCs and bone marrow-derived MSCs demonstrated a clear functional advantage of hCMSCs in the restoration of epithelial permeability in vitro, as illustrated in supplemental online Figure 10.

Expression of Growth Factors by hCMSCs

We have previously shown that the therapeutic effect of BM-MSCs is related in part to the production of growth factors such as KGF [22]. Therefore, we measured the release of several growth factors and other soluble factors by hCMSCs. Gonadotropin was not found in hCMSC-conditioned medium. Measurements of levels of HGF, FGF-β, KGF, and ANG-1 in conditioned medium of hCMSCs compared with BM-MSCs demonstrated the presence of abundant amounts of the growth factors after 5–7 days of culture, and levels of the growth factors were significantly higher in hCMSCs compared with BM-MSC cultures (Fig. 7A). To determine whether the therapeutic effect of hCMSCs is related to their secretory ability, we used Transwell coculture of injured lung epithelial cells and hCMSCs. hCMSCs were compared with BM-MSCs, both of which were added to parallel culture systems after damage, either under conditions of direct cell-to-cell contact (Fig. 7B) or without direct cell-to-cell contact (Transwell). To confirm presence of hCMSCs in coculture, we labeled hCMSCs with the vital dye PKH-26. Figure 7B demonstrates location of hCMSCs in Transwell clusters 24 hours following their application to the apical side of the epithelial layers. When added on the top of damaged lung epithelial layers or to the bottom well (without cell contact) in the Transwell culture system, hCMSCs had a marked effect on restoration of the TER (Fig. 7C). Effects of either direct cell-cell contact between epithelial cells and hCMSCs or indirect action (without cell contact) were not different between the two. Also, the effects of hCMSCs were significantly more pronounced than the effect of the BM-MSCs (Fig. 7C2, 7C3). This observation is consistent with the higher paracrine activity of hCMSCs compared with BM-MSCs. To confirm the involvement of paracrine mechanisms, siRNA blockade of several growth factors (HGF, FGF-β, and KGF) was performed in these cells. hCMSCs were transfected for 24 hours prior to coculture with damaged Calu-3 cells. hCMSCs transfected with siRNAs targeted for any one of the three growth factors reduced the effect by 20%–30% compared with lines transfected with noncoding siRNAs. Transfection of hCMSCs with a combination of all three siRNAs significantly reduced the positive effect of the coculture (Fig. 7C4). These data support our earlier hypothesis that the effect of MSCs on restoration of epithelial permeability is due in part to the paracrine effects of growth factors, including but not limited to HGF, FGF-β, and KGF.

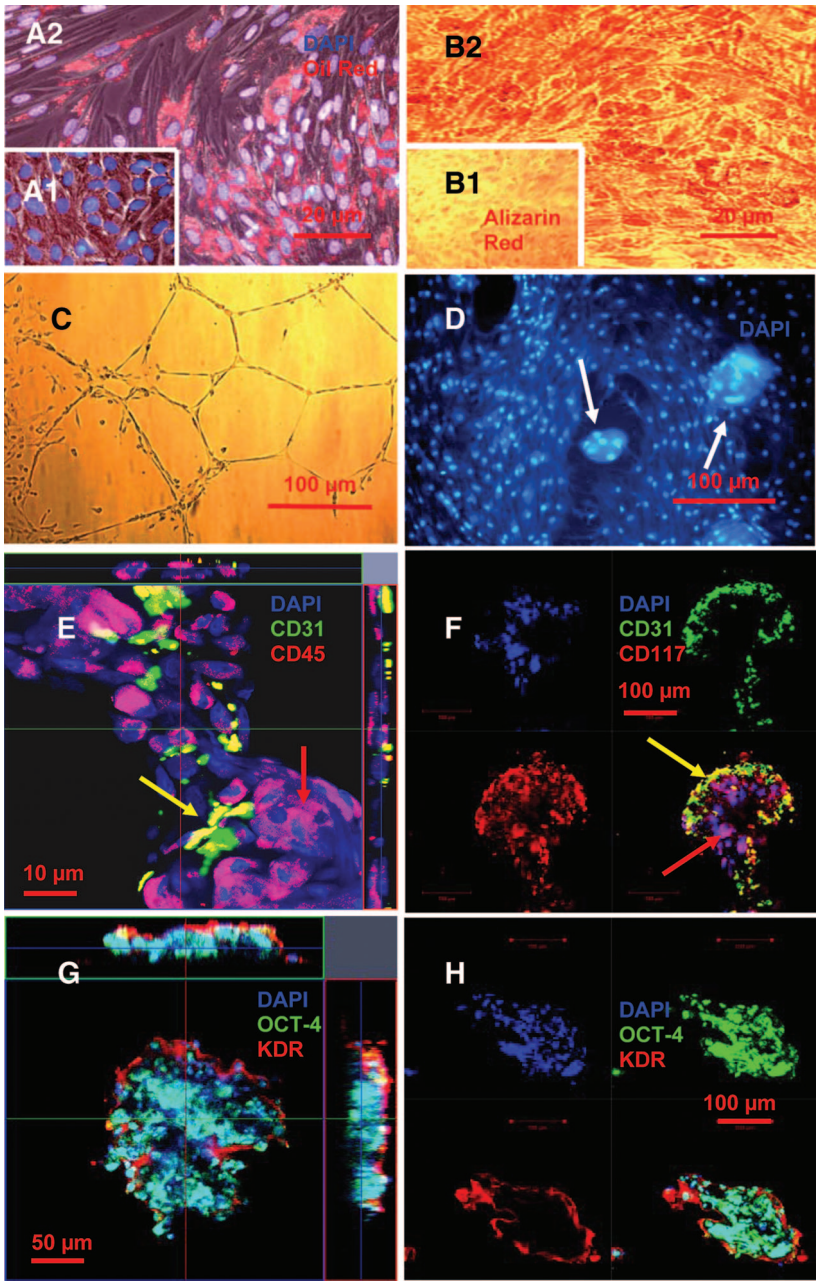

Figure 4. Mesodermal differentiation of chorionic mesenchymal stem cells. **(A):** Adipogenic differentiation, bright light image (Oil Red staining for fat, red). **(A1):** Control cells. **(A2):** Cells grown in adipogenic medium. **(B):** Osteoblast differentiation, bright light image (red staining with alizarin red for calcium precipitates in cells). **(B1):** Control cells. **(B2):** Cells grown in osteogenic medium. **(C):** Capillary-like structures and capillary network formed by chorionic cells grown on Matrigel in standard growth medium. Phase-contrast image. **(D):** Chorionic mesenchymal stem cells grown in Methocult medium supporting hematopoietic differentiation, staining for nuclei with DAPI (blue). Two distinct cell populations were present: cells attached to the surface formed a monolayer, and cells not attached to the surface grew as loose spherical bodies (arrows). **(E, F):** Chorionic mesenchymal stem cells grown on media stimulating endothelial differentiation (Matrigel) for 5 days, followed by the addition of Methocult medium for next 7 days. Immunofluorescent images. Two distinct cell populations were present: cells attached to the Matrigel substrate had an endothelial phenotype, and cells not attached to the surface (bodies) showed phenotype of blood or undifferentiated cells. **(E):** Confocal microscopy *z*-stack three-dimensional image. Staining for CD45 (phycoerythrin [PE], red) and for CD31 (fluorescein isothiocyanate [FITC], green); costaining for nuclei with DAPI. Surface cells displayed CD31 (endothelial cell marker) or both CD31 and CD45 leukocyte marker (yellow arrow). Cells inside spherical bodies expressed CD45 but not CD31 (red arrow). **(F, H):** Split confocal images. Upper left: blue channel (nuclei); upper right: green channel; lower left: red channel; lower right: combined image. **(F):** Staining for CD117 (PE, red) and for CD31 (FITC, green); costaining for nuclei with DAPI (blue). Surface attached cells displayed CD31 (endothelial cell marker, yellow arrow). Cells inside spherical bodies expressed CD117 but not CD31 (red arrow). **(G):** Embryoid body-like structures, grown on media stimulating endothelial differentiation (Matrigel) for 5 days. Cells inside the embryoid body expressed OCT-4 (green), whereas cells at the outer layer differentiated into endothelial cells (expression of KDR, red). Confocal microscopy *z*-stack image: immunostaining for KDR (AF663, red) and for OCT-4 (FITC, green); costaining for nuclei with DAPI. **(H):** Same as **(G)**: image of embryoid body demonstrating expression of KDR on the outer layer of the embryoid body structure and extensive expression of OCT-4 in cells inside the embryoid body structure. Additional split images are shown in supplemental online Figure 4. Abbreviations: DAPI, 4′,6-diamidino-2-phenylindole; KDR, type III receptor tyrosine kinase, also known as vascular endothelial growth factor receptor 2.

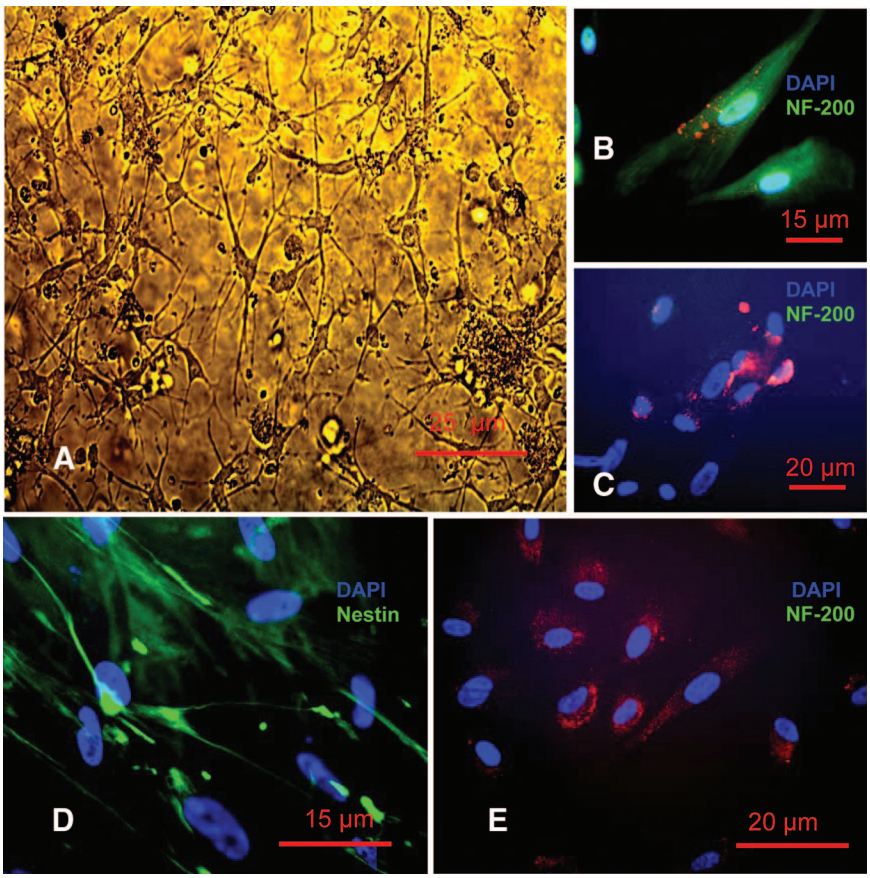

Figure 5. Ectodermal differentiation of chorionic mesenchymal stem cells. **(A):** Overall appearance of sprouting neuron-like cells upon culture in nerve growth factor (NGF)-containing medium. Differential interference contrast microscopy image. **(B–E):** Following culture in neurogenic medium containing 10^{-8} M NGF, different cell lines expressed multiple markers of neurons and glial cells. Combined images for green, blue, and red channels; red nonspecific fluorescence shows red-fluorescent cell inclusions. Red channel images are shown to demonstrate specificity of green fluorescence. **(B):** Induced expression of Neurofilament-200 (fluorescein isothiocyanate, green), nuclear costaining DAPI (blue). **(C):** Isotype antibody staining for Neurofilament-200 in cells cultured in neurodifferentiation medium, nuclear costaining DAPI (blue). **(D):** Induced expression of Nestin (green), nuclear costaining DAPI (blue) **(E):** Negative control: no expression of Neurofilament-200, in chorionic stem cell line cultured in medium without NGF. Staining for Neurofilament-200 (green), nuclear costaining DAPI (blue). Abbreviations: DAPI, 4′,6-diamidino-2-phenylindole; NF, Neurofilament.

Acute Toxicology and Tumorigenicity

Injection of 0.25×10^6 hCMSCs i.v. into the jugular vein and 1×10^6 hCMSCs i.p. was well tolerated by mice. No immediate signs of cardiovascular distress were observed, and none of the mice died. During further observation, no signs of distress, pain, or weight loss were noted. Possible tumor or teratoma formation was studied by focal injection of 1 million cells in 10 animals; in half of these cases, cells were cultured on Matrigel prior to injection. Observations up to 1 year did not show teratoma formation at the site of injection or other tumors with human cells. No tumors containing human cells were observed in the body or internal organs.

Engraftment in Immunodeficient Mice

Engraftment of hCMSCs into various organs was determined after 2–6 months by PCR for the human β-globin gene and by FISH for the human Y chromosome. Immunostaining for cytokeratins 18 and 20 (intestine); pancytokeratin, albumin, and α-fetoprotein (liver hepatocytes); Neurofilament-200 (neurons); and S-100 (glial cells) in the brain was done in subsequent organs. Cells positive for the human Y chromosome were found in almost all organs. Their presence was documented in the intestine, in the lungs, in the liver, and in the brain, as illustrated in supplemental online Figure 11. Quantification based upon presence of Y chromosome-positive cells demonstrated that 10 of 12 mice were grafted. The percentage of Y chromosome-positive cells was highest in the liver (0.01%–0.1%). Quantification of engraftment was done based upon PCR results for all studied organs in eight mice, as shown in supplemental online Table 3.

Discussion

In this report, stem cell lines obtained from the chorion (hCMSCs) of human placenta are shown to have several features: (a) hCMSCs could remain viable and propagate for more than 100 doublings (55 passages); (b) cells can be differentiated in vitro into neuron-like cells (ectoderm), adipocytes, osteoblasts, endothelial-like cells (mesoderm), and hepatocytes (endoderm); (c) cells from placental tissue form embryoid body-like spherical structures; and (d) cells secrete abundant amounts of multiple growth factors, including HGF, FGF-β, and angiopoietin 1, and facilitate recovery of epithelial barrier function in in vitro and ex vivo human lung models. hCMSCs are similar to the previously described placental cell lines [6–20] as they express markers of pluripotent stem cells (OCT-4, NANOG, SSEA-3) and surface markers of mesenchymal cells (CD73, CD90, CD105). As hCMSCs maintain telomere length and lack telomerase activity, these cells likely use alternative mechanisms of telomere lengthening, which are discussed in detail by Muntoni and Reddel [23]. We report only limited characterization of the mechanisms of telomere lengthening, but our data clearly indicate that this feature of hCMSCs distinguishes them from human embryonic cells.

Our data are in agreement with prior [18] and recent [24] reports demonstrating that placental cells express some embryonic stem cell markers. Cells derived from placenta demonstrated proximity to pericyte origin [25] and were shown to differentiate into a neuron-like phenotype [26], similar to our results. In a mouse model of fibrotic lung injury, placental cells

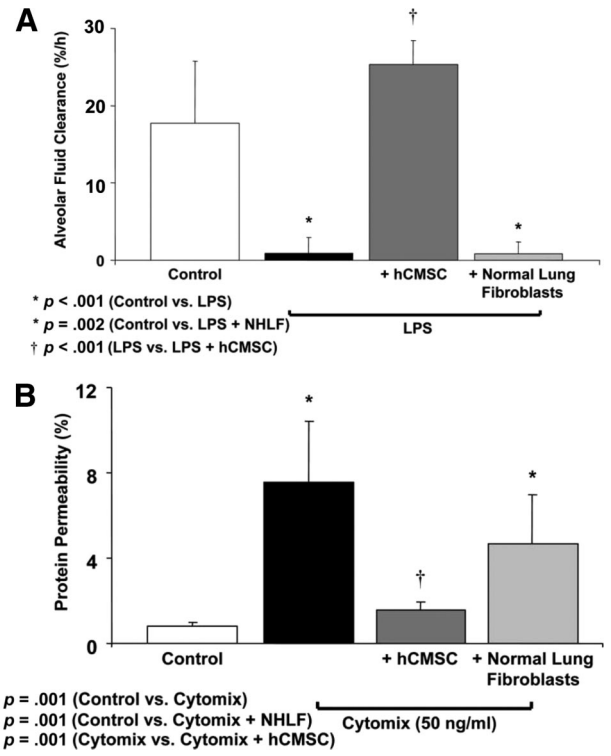

Figure 6. Chorionic mesenchymal stem cells demonstrated high therapeutic activity in the injured lung. **(A):** hCMSCs restored by the decrease in alveolar fluid clearance in the lung lobe injured by endotoxin (lipopolysaccharide *Escherichia coli* [LPS]). The addition of hCMSCs (5×10^6 cells) given 1 hour following endotoxin injury (LPS + hCMSCs) fully restored alveolar fluid clearance in the lung lobe to control values at 4 hours. $n = 3–8$. **(B):** hCMSCs restored permeability to albumin in primary cultures of human alveolar epithelial type II cells injured by an inflammatory insult. Forty-eight hours after confluence of epithelium was achieved, human alveolar epithelial type II cells were exposed to cytomix with and without hCMSCs grown in the bottom chamber. The cytomix (50 ng/ml) increased epithelial permeability. The presence of hCMSCs (250,000 cells per well) grown on the bottom chamber reversed the increase in protein permeability induced by cytomix. $n = 3–6$. Abbreviations: hCMSC, human chorionic mesenchymal stem cell; NHLF, normal human lung fibroblasts.

had a therapeutic effect [27], which is also in line with our observations. The amnion and chorion of human term placentas contain multiple populations of different types of primitive stem cells. We derived lines by mechanical isolation from a specific type of cell growth in embryoid body-like spherical structures; therefore, the existence of subpopulations cannot be excluded. As the chorion is the largest part of placental outer membrane, it is the most attractive source of therapeutically valuable stem cells.

Several previous reports [11, 28, 29] demonstrated that in many cases a substantial amount of the cells cultured out of the placenta, or all of them, were of maternal origin. Cells in our cultures derived from male placentas were positive for the human Y chromosome, although this does not exclude a possibility of presence of maternal cells. We did not specifically aim to obtain or compare fetal versus maternal cells in this study and therefore did not do complete cytogenetic analyses. Prior studies that found predominantly maternal cells in culture did not separate decidual membranes from placenta [28], so the presence of maternal cells is not unexpected. We tried a different approach to minimize such contamination: first by tissue digestion with perfusion and then by selection of rapidly growing embryoid body-like cell colonies. Our perfusion-digestion protocol was used to facilitate isolation of cells of a fetal origin. Digestion via perfusion allows the delivery of enzymes only to the fetal part of placental barrier. In our opinion, perfusion-digestion methods are physiologically grounded technical procedures to obtain enriched fetal cells from the chorion and avoid decidual maternal cell contamination, to the extent the natural continuum of the fetal circulation in placenta allows it. The embryoid body-derivation step allowed us to naturally select the most fast-growing colonies. In our opinion, it is likely that the fetal cells would have superior growth characteristics and expression of embryonic stem cell markers compared with maternal cells. As FISH for Y chromosome does not allow elimination of a possible admixture of maternal cells, their presence in our lines could not be completely ruled out in this study. Our future studies will be aimed at further development of perfusion-digestion (or perfusion with receptor blocker compounds) to optimize yield of pure fetal cell populations.

The perfusion approach seems to be valuable for several reasons, including obtaining enriched populations of fetal cells and further placenta cryopreservation. It is currently not known how to effectively preserve the whole placenta or large amounts of placental material for future use. At first glance, it seems that the placenta could be processed at the time of birth to obtain cells and that subsequently cells could be cryopreserved. Currently, the costs required to digest a whole placenta are extremely high, as relatively large amounts of digestive enzymes are required. Placenta needs to be processed soon after delivery, which limits shipment of placenta to a specialized facility without proper means of preservation. Harvesting stem cells from the placenta seems to be economically viable only when the cells are specifically required for use. Therefore, initial cryostorage of whole placenta with future derivation of stem cells on an as-needed basis is a more logical approach. Placentas could be stored in banks similar to cord blood units. Therefore, development of efficient means of local preservation and storage, like perfusion means, is required to make the optimal use of this important resource, which will be the aim of our future experiments.

We further tested the human therapeutic potential of hCMSCs using *Escherichia coli* endotoxin to induce acute lung injury in an ex vivo human lung. Instillation of endotoxin into one lung lobe produced severe impairment of alveolar fluid clearance— one of the major functional properties of alveolar-blood barrier. This represents the results of an inflammatory reaction to endotoxin, as indicated by increased neutrophil flux and enhanced levels of the inflammatory cytokines IL-1β, TNFα, and IL-8 in alveolar fluid. Alveolar fluid clearance is determined by epithelial barrier integrity and regulated by multiple proteins and signaling cascades modulating tight junctions of the epithelial cells, as well as the function of sodium pumps and water channels. The inflammatory reaction at the level of the alveolar epithelial barrier is very complex and is associated with deterioration of barrier integrity. At the same time, endotoxin toxicity results in downregulation of expression and transport of proteins involved in active ion transport. Therefore, pleiotropic effect of placental stem cells, as shown in our study in whole human lung and isolated alveolar type II cell cultures, restored cellular machinery of protein synthesis, transport, and intercellular integrity.

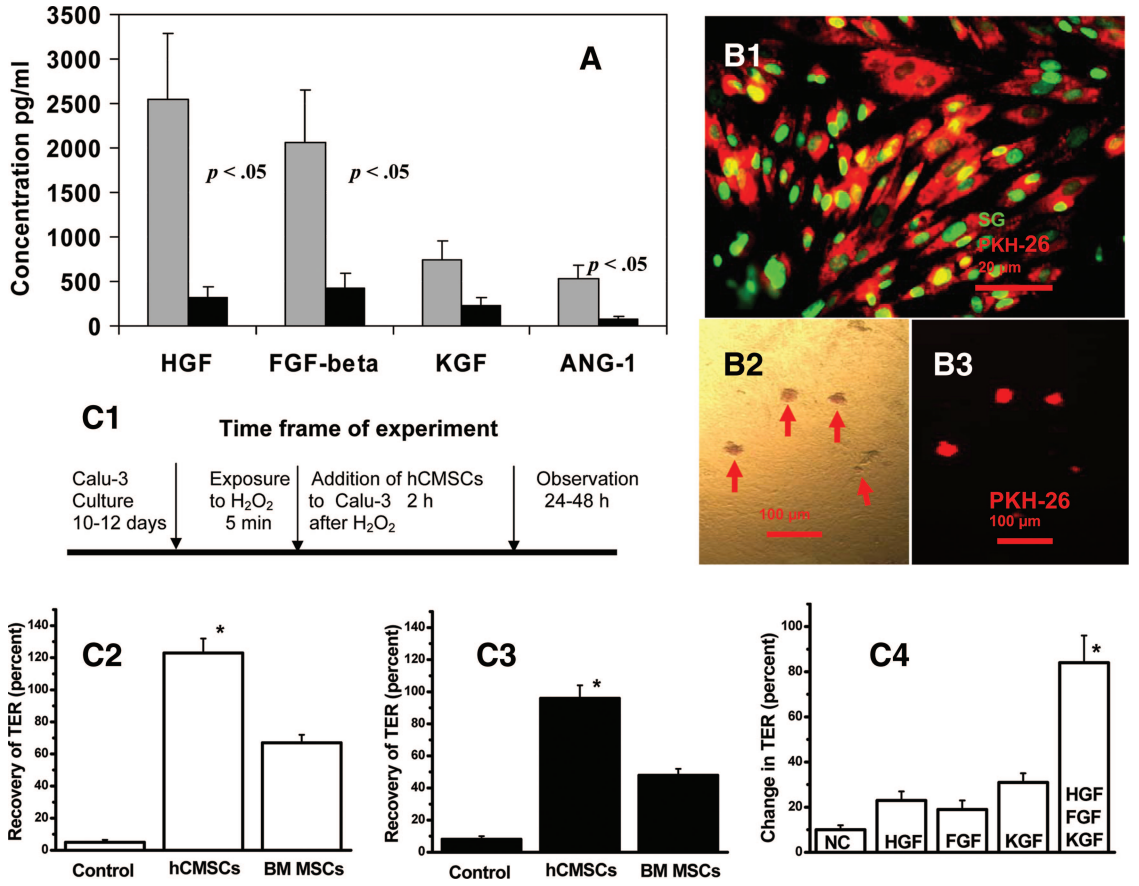

Figure 7. Therapeutic effect of chorionic mesenchymal stem cells is related to high paracrine activity. **(A):** hCMSCs released abundant quantities of multiple growth factors. Shown are levels of HGF, FGF-β, KGF, and ANG-1 in cell culture medium of chorionic cells (gray) as compared with MSCs derived from human bone marrow (black). **(B):** Coculture of lung bronchoepithelial cells and hCMSCs in the Transwell system. Fluorescent **(B1, B3)** and differential interference contrast microscopy (DIC) **(B2)** images. **(B1):** For identification purposes, hCMSCs were stained in culture with the red fluorescent vital dye PKH-26 (Sigma-Aldrich) and the green nuclear dye SYBR Green (Invitrogen). **(B2):** Calu-3 lung bronchoepithelial cells were grown as inserts on Transwell supports. DIC image after application of PKH-26-labeled hCMSCs on the apical surface. Clusters of hCMSCs are indicated with red arrows. **(B3):** Fluorescent image corresponding to that shown in **(B2)**. Clusters of red hCMSCs are clearly visible. **(C):** hCMSCs produced reparative effect on injured lung bronchial epithelial layer. **(C1):** Time frame of experiment. Following 10–12 days of culture on air-liquid interface on a 0.4-μm pore size Transwell support, Calu-3 layers achieved a TER of 800–1,000 $\Omega \times cm^2$. Cells were exposed to hydrogen peroxide (2 mM) for 5 minutes. Two hours later, hCMSCs, BM-MSCs, or A549 cells (negative control) were either applied to the apical side or added to the lower well of a Transwell system (balsolateral side) at concentrations of 10^5 cells per cm^2. TER was measured in 12-hour periods for 24–48 hours. **(C2):** Recovery of TER at 24 hours following apical (direct cell-cell contact) application of hCMSCs, BM-MSCs, or A549. Application of A549 cells did not restore TER (control). Restoration of TER by hCMSCs was significantly higher than that by BM-MSCs (*, $p < .05$). **(C3):** Recovery of TER at 24 hours following basal application (paracrine effect) of hCMSCs, BM-MSCs, or A549. Application of cells to the basal compartment of a Transwell system prevented cell-cell contact, and the effects were due to paracrine action. Application of A549 cells did not restore TER (control). Restoration of TER by hCMSCs was significantly higher than that by BM-MSCs (*, $p < .05$). **(C4):** Small interfering RNA (siRNA) blockage of HGF, FGF, and KGF in hCMSCs prevented restoration of injured airway epithelium. hCMSCs were subject to treatment with siRNA for HGF, FGF-2, or KGF prior to application to basolateral side of Calu-3 layers. Treatment with each individual siRNA produced a moderate effect on the capability of hCMSCs to restore injured lung epithelial cells by paracrine mechanisms. Treatment of hCMSCs with siRNA for all three factors together produced a significant reduction in their paracrine effect ($p < .05$). Noncoding siRNAs were used as negative control. Abbreviations: ANG, angiopoietin; BM MSC, bone marrow-derived mesenchymal stem cell; FGF, fibroblast growth factor; hCMSC, human chorionic mesenchymal stem cell; HGF, hepatocyte growth factor; KGF, keratinocyte growth factor; NC, negative control; SG, SYBR Green (cyanine nuclear binding stain); TER, transepithelial electrical resistance.

To study the effects of hCMSCs on lung tissue regeneration in more detail, we used a model of bronchoepithelial cells grown on an air-liquid interface [21]. Oxidative injury by hydrogen peroxide rapidly decreased transepithelial electrical resistance. Our initial hypothesis was that hCMSCs may exert paracrine effects. To test this hypothesis, we compared the effects of direct cell-cell contact to the effects of cells placed in coculture conditions that prevented direct cell-cell contact. In these experiments, we found that hCMSCs were highly effective in the restoration of barrier properties of injured bronchial epithelium both with and without cell-cell contact. Moreover, hCMSCs were significantly more effective than BM-MSCs, which correlated well with the level of several growth factors secreted by hCMSCs as compared with BM-MSCs. Using siRNA for such factors as HGF, FGF, and KGF, we demonstrated that simultaneous silencing of all of these genes reduced the functional effect of hCMSCs by 85%. We, therefore, conclude from these data that functional paracrine effect of hCMSCs was closely related to secretion of these and possibly other growth factors. Pleiotropic effect of these growth factors and cytokines resulted in enhanced restoration of epithelial barrier function [30]. Of many growth factors, hepatocyte growth factor was very intensively synthesized and secreted by

hCMSCs. HGF is a growth, motility, and morphogenic factor. Its primary targets are epithelial and endothelial cells in wound healing [30]. HGF regulates cell processes by activating a tyrosine kinase signaling cascade through the proto-oncogenic c-Met receptor. HGF belongs to the plasminogen subfamily of S1 peptidases, although it does not have protease activity. HGF is known to be a highly important cytokine in lung morphogenesis and repair [31]. High levels of HGF and FGF could be expected based upon the current understanding that cells of the placenta, such as trophoblasts, are close to cancer cells in their level of activity of some signaling circuits, such as epidermal growth factor (EGF)/EGF receptor, HGF/c-Met, and vascular endothelial growth factor/VEGFR [32]. FGF2 (bFGF), another cytokine found to be highly secreted by hCMSCs, is a member of the fibroblast growth factor family. Basic fibroblast growth factor is present in basement membranes during both regeneration of normal tissues and tumor development [33]. The role of KGF released by MSCs was recently emphasized in our study [22], which demonstrated that this growth factor released by MSCs introduced to the injured lung is a very potent modulator of epithelial repair and recovery of altered alveolar fluid clearance.

There are several risks associated with stem cell-based therapies [34]. Tumor growth or stimulation of growth of a tumor by MSCs is the most well-recognized risk factor. As our results indicated, hCMSCs did not form tumors or, specifically, teratomas in immunocompromised and irradiated animals. This is an important practical consideration, confirming established data that fetal cells, unlike embryonic cells, do not form tumors. Recognized options to mitigate the risk of tumor formation include the induction of differentiation in cell culture, sorting of cells or introduction of a suicide gene, chemotherapy, and cell-specific antibody administration [34]. Considering the fact that therapies for life-threatening conditions such as acute lung injury are likely to be based upon engraftment-independent modes of stem cell action [22], a balance could be achieved between a very high mortality risk (up to 40%) in such conditions and a low risk of tumor development by fetal cells. Also, we did not observe immediate cell toxicity upon i.v. or i.p. administration.

Another mode of hCMSC action may be related to the immunomodulatory effect. We did not specifically aim to investigate this aspect in our study, as hCMSCs demonstrated a lack of HLA-DR expression, and both ESC-derived cells and MSCs are known to be immune-privileged. However, the immune effect of MSCs has been described in multiple reports. MSCs have been described to suppress T-cell proliferation, inhibit differentiation of monocytes, affect function of dendritic cells, inhibit TNF production, increase IL-10 production, and inhibit proliferation and cytotoxicity of resting natural killer cells and their cytokine production [34]. Our studies in an in vitro epithelial culture model did not include any immunocompetent cells. Isolated human lung, however, was perfused with fresh human blood, and endotoxin was used to injure the lung. We cannot exclude immune effects of hCMSCs in our study, although this short-term ex vivo model is unlikely to largely depend upon long-term immunological reactions. Our prior study in isolated human lung [22] demonstrated that the primary effect of bone marrow MSCs was also related to release of KGF, minimizing the possibility of immunological effects in this model. Detailed characterization of specific immunomodulatory effects of hCMSCs remains a subject of our further study, as different human-specific models ought to be used for such purposes.

Conclusion

Multipotent hCMSCs possess several clear advantages over other types of stem cells for human therapy. First, hCMSCs could be obtained from fetal precursors, and if confirmed as such, retain more plasticity than adult cells with shorter telomeres. Furthermore, as placentas are usually discarded, the source of hCMSCs is abundant and noncontroversial. Second, hCMSCs produce large amounts of growth factors, thus acting as potent paracrine modulators, and do not make tumors upon transplantation in immunocompromised animals. Primary hCMSCs could be obtained in large numbers, which would be important for the production of therapeutic products. This study is the first to demonstrate a potential therapeutic effect of human chorionic mesenchymal stem cells in a human organ model of acute lung injury and their potential for further use in clinical trials.

Acknowledgments

We greatly appreciate the extraordinary support for this project, involvement, and encouragement by Dr. Bruce Ames, a professor at the University of California, Berkeley, and a senior scientist, Children's Hospital Oakland Research Institute (CHORI). This work was supported in part by funds from the Jean J. Deleage Ph.D. and Josette Deleage Foundation, Bay View Eagles Lodge, CHORI Jordan Family Foundation (to V.B.S.), CHORI Ventures, NIH HL-070583, 1R43HL108327, 1R43DK091963 (to F.A.K.), NIH HL-51856 and HL-51854 (M.A.M.), NIH HL-093026 (to J.W.L.), and the Foundation of Anesthesia Education & Research (to J.W.L.). We thank Dr. B. Lubin for support from CHORI. We are grateful to the Northern California Transplant Donor Network for assistance in obtaining human research lungs. Some of the materials were provided by the Tulane Center for Gene Therapy (NIH Grant P40RR017447). hESC and iPSC lines were a kind gift of C. Tahimic and Pieter De Jong (CHORI) and E. Bashkirova (Stanford University).

Disclosure of Potential Conflicts of Interest

The authors indicate no potential conflicts of interest.

Author Contributions

I.N. and S.E.: performed cell culture studies; J.W.L.: performed lung studies; E.S.: performed reverse transcription and real-time PCR; D.K. and E.B.: performed histology studies; W.G.: performed engraftment studies in mice; X.F.: performed lung cell culture studies; M.A.M. and F.A.K.: planned experiments, reviewed manuscript; V.B.S.: planned experiments, performed placental studies, cell culture studies, immunohistology.

References

1 Serikov V, Hounshell C, Larkin S et al. Human term placenta as a source of hematopoietic cells. Exp Biol Med (Maywood) 2009;234:813–823.

2 Gekas C, Dieterlen-Lievre F, Orkin S et al. The placenta is a niche for hematopoietic stem cells. Dev Cell 2005;8:365–375.

3 Robin C, Bollerot K, Mendes S et al. Human placenta is a potent hematopoietic niche containing hematopoietic stem and progenitor cells throughout development. Cell Stem Cell 2009;5:385–395.

4 Bárcena A, Kapidzik M, Muench M et al. The human placenta is a hematopoietic organ during the embryonic and fetal periods of development. Dev Biol 2009;327:24–33.

5 Levi B, Morrison S. Stem cells use distinct self-renewal programs at different ages. Cold Spring Harb Symp Quant Biol 2008;73:539–553.

6 De Coppi P, Bartsch G, Siddiqui M et al. Isolation of amnionic stem cell lines with potential for therapy. Nat Biotechnol 2007;25:100–106.

7 Fukuchi Y, Nakagima H, Sugiyama D et al. Human placenta-derived cells have mesenchymal stem/progenitor cell potential. Stem Cells 2004;22:649–658.

8 Matikainen T, Laine J. Placenta: An alternative source of stem cells. Toxicol Appl Pharmacol 2005;207(2 suppl):544–549.

9 Yen BL, Huang HI, Chien CC et al. Isolation of multipotent cells from human term placenta. Stem Cells 2005;23:3–9.

10 Sakuragawa N, Kakinuma K, Kikuchi A et al. Human amnion mesenchyme cells express phenotypes of neuroglial progenitor cells. J Neurosci Res 2004;78:208–214.

11 In 't Anker PS, Scherjon SA, Kleijburg-van der Keur C et al. Isolation of mesenchymal stem cells of fetal or maternal origin from human placenta. Stem Cells 2004;22:1338–1345.

12 Portmann-Lanz C, Schoeberlein A, Huber A et al. Placental mesenchymal stem cells as potential autologous graft for pre- and perinatal neuroregeneration. Am J Obstet Gynecol 2006;194:664–673.

13 Wolbank S, Peterbauer A, Fahrner M et al. Dose-dependent immunomodulatory effect of human stem cells from amniotic membrane: A comparison with human mesenchymal stem cells from adipose tissue. Tissue Eng 2007;13:1173–1183.

14 Soncini M, Vertua E, Gibelli L et al. Isolation and characterization of mesenchymal cells from human fetal membranes. J Tissue Eng Regen Med 2007;1:296–305.

15 Wei J, Zhang T, Kawa S et al. Human amnion-isolated cells normalize blood glucose in streptozotocin-induced diabetic mice. Cell Transplant 2003;12:545–552.

16 Alviano F, Fossati V, Marchionni C et al. Term amniotic membrane is a high throughput source for multipotent mesenchymal stem cells with the ability to differentiate into endothelial cells in vitro. BMC Dev Biol 2007;7:11.

17 Zhao P, Ise H, Hongo M et al. Human amniotic mesenchymal cells have some characteristics of cardiomyocytes. Transplantation 2005;79:528–535.

18 Parolini O, Alviano F, Bagnara G et al. Isolation and characterization of cells from human term placenta: Outcome of the First International workshop on placenta derived stem cells. Stem Cells 2008;26:300–311.

19 Bailo M, Soncini M, Vertua E et al. Engraftment potential of human amnion and chorion cells derived from term placenta. Transplantation 2004;78:1439–1448.

20 Zhang X, Mitsuru A, Igura K et al. Mesenchymal progenitor cells derived from chorionic villi of human placenta for cartilage tissue engineering. Biochem Biophys Res Commun 2006;340:944–952.

21 Serikov V, Choi H, Chmiel KJ et al. Activation of extracellular regulated kinases is required for the increase in airway epithelial permeability during leukocyte transmigration. Am J Respir Cell Mol Biol 2004;30:261–270.

22 Lee J, Xiaohui Fang, Gupta N et al. Potential application of mesenchymal stem cells in acute lung injury. Proc Natl Acad Sci USA 2009;106:16357–16362.

23 Muntoni A, Reddel R. The first molecular details of ALT in human tumor cells. Hum Mol Genet 2005;14:R191–R196.

24 Poloni A, Rosini V, Mondini E et al. Characterization and expansion of mesenchymal progenitor cells from first-trimester chorionic villi of human placenta. Cytotherapy 2008;10:690–697.

25 Castrechini N, Murthi P, Gude N et al. Mesenchymal stem cells in human placental chorionic villi reside in a vascular niche. Placenta 2010;31:203–212.

26 Portmann-Lanz CB, Baumann MU, Mueller M et al. Neurogenic characteristics of placental stem cells in preeclampsia. Am J Obstet Gynecol 2010;203:399.e1–e7.

27 Cargnoni A, Gibelli L, Tosini A et al. Transplantation of allogeneic and xenogeneic placenta-derived cells reduces bleomycin-induced lung fibrosis. Cell Transplant 2009;18:405–422.

28 Barlow S, Brooke G, Chatterjee K et al. Comparison of human placenta- and bone marrow-derived multipotent mesenchymal stem cells. Stem Cells Dev 2008;176:1095–1107.

29 Semenov OV, Koestenbauer S, Riegel M et al. Multipotent mesenchymal stem cells from human placenta: Critical parameters for isolation and maintenance of stemness after isolation. Am J Obstet Gynecol 2010;2022:193.e1–193.e13.

30 Crosby L, Waters C. Epithelial repair mechanisms in the lung. Am J Physiol Lung Cell Mol Physiol 2010;298:L715–L731.

31 Ware L, Matthay M. Keratinocyte and hepatocyte growth factors in the lung: Roles in lung development, inflammation, and repair. Am J Physiol Lung Cell Mol Physiol 2002;282:L924–L940.

32 Ferretti C, Bruni L, Dangles-Marie V. Molecular circuits shared by placental and cancer cells, and their implications in the proliferative, invasive and migratory capacities of trophoblasts. Hum Reprod Update 2007;13:121–141.

33 Itoh N, Ornitz D. Fibroblast growth factors: From molecular evolution to roles in development, metabolism and disease. J Biochem 2011;149:121–130.

34 Herberts CA, Kwa MS, Hermsen HP. Risk factors in the development of stem cell therapy. J Transl Med 2011;9:29–35.

See www.StemCellsTM.com for supporting information available online.